

Optimal FALQON for Quantum Approximate Optimization via Layer-wise Parameter Tuning

Michael Mancini and Shabnam Sodagari, *Senior Member, IEEE*

Computer Engineering & Computer Science
California State University, Long Beach, CA 90840
michael@mancini.institute; shabnam@csulb.edu

Abstract—Feedback-based adaptive quantum optimization (FALQON) is a promising approach for solving combinatorial problems on noisy intermediate-scale quantum (NISQ) devices, requiring only single circuit evaluations per layer. However, standard FALQON relies on fixed hyperparameters that severely limit convergence speed, requiring hundreds to thousands of layers for acceptable solutions. This paper proposes Optimal FALQON, an optimization-based formulation that treats the per-layer time step (δ_k) and scaling factor (M_k) as decision variables optimized via classical methods. We present a comprehensive empirical study on all 94 non-isomorphic 3-regular graphs with 12 vertices, comparing Optimal FALQON with standard FALQON and multiple QAOA variants. Results demonstrate statistically significant improvements in success probability, evaluation efficiency, and depth-normalized cost across the evaluated benchmarks. Furthermore, initializing QAOA with parameters from Optimal FALQON yields superior warm-start performance compared to fixed initialization.

Index Terms—Quantum optimization, variational quantum algorithms, FALQON, QAOA, parameter optimization, NISQ

I. INTRODUCTION

Quantum optimization algorithms such as the Variational Quantum Eigensolver (VQE), the Quantum Approximate Optimization Algorithm (QAOA), and the recently proposed Feedback-Based Adaptive Quantum Optimization (FALQON) have emerged as promising tools for solving combinatorial problems on noisy intermediate-scale quantum (NISQ) devices [1]–[5].

QAOA relies on classical optimization of parameters γ_k and β_k at each layer, which can require extensive circuit evaluations. Here, γ_k is the rotation angle applied to the problem (cost) Hamiltonian at layer k , and β_k is the rotation angle applied to the driver (mixer) Hamiltonian at layer k . In contrast, FALQON provides an analytically derived scheme requiring only a single circuit evaluation per layer. However, standard FALQON exhibits a critical limitation: it requires hundreds or thousands of layers to achieve satisfactory convergence because the fixed time step δ and gain factor w must be chosen conservatively to guarantee stability [4], [5]. This inefficiency is particularly problematic on current hardware where circuit depth and shot budgets are severely constrained.

Current superconducting quantum hardware faces gate-error limitations, with representative single-qubit gate errors around 10^{-3} and two-qubit gate errors in the 10^{-3} to 10^{-2} range [6], [7]. Additionally, execution costs for off-premises quantum

hardware remain on the order of \$10 per execution [8], [9], leading to several hundreds of dollars per solution.

Recent FALQON literature demonstrates strong sensitivity to step and gain choices. The original formulation uses fixed-step implementations with fixed gain ($w = 1$), while subsequent works introduce analytical modifications such as time-rescaling factors and robust gain regularization [10], [11]. These extensions effectively adjust per-layer step and scaling terms, suggesting that direct layer-wise optimization of both parameters could substantially improve practical performance.

A. Contributions

This paper makes the following contributions:

- **Optimal FALQON:** An optimization-based formulation treating the per-layer time step δ_k and scaling term M_k as decision variables, optimized via the Powell method.
- **Comprehensive Benchmarking:** A comprehensive evaluation framework (Python/PennyLane) benchmarking Optimal FALQON against standard FALQON and multiple QAOA variants on all 94 non-isomorphic 3-regular graphs with $N = 12$ vertices.
- **Statistical Evidence:** Paired Wilcoxon signed-rank tests with Holm correction demonstrating statistically significant improvements in success probability and efficiency metrics.
- **Warm-Start Analysis:** Quantitative assessment showing that initializing QAOA with parameters from Optimal FALQON yields substantial performance improvements compared to fixed initialization and warm-starts from standard FALQON.

The organization of this paper is as follows. Section II provides background on quantum systems, the MaxCut problem benchmark, and existing optimization algorithms (QAOA, QAOA-MA, and standard FALQON), along with foundational statistical testing methodology. Section III introduces the Optimal FALQON formulation, derives the per-layer parameter equations, and justifies the selection of the Powell optimizer for noisy quantum optimization. Section IV presents comprehensive simulation results across all 94 graph instances and depths 1–10, including success probability distributions, efficiency metrics, and statistical significance tests. Section V discusses key insights regarding dynamic per-layer tuning, cross-method comparisons, and warm-start synergies. Finally,

Section VI concludes with a summary of findings and implications for NISQ-era quantum optimization.

II. RELATED WORK AND BACKGROUND

A. Quantum Optimization on NISQ Devices

Quantum optimization algorithms have attracted significant interest for solving combinatorial problems on near-term quantum hardware. The Variational Quantum Eigensolver (VQE) [1] pioneered the variational approach to hybrid quantum-classical computation, becoming a foundational method for quantum chemistry simulations [2]. The Quantum Approximate Optimization Algorithm (QAOA) extends this framework to combinatorial optimization, providing a gate-depth-efficient approach [3] that has become a standard benchmark for near-term quantum algorithms.

Recent advances in feedback-based quantum control have led to the development of FALQON [4], which provides an analytically-derived optimization scheme requiring minimal circuit evaluations. Building on FALQON’s foundation, subsequent work introduced time-rescaling improvements [10] and robust gain regularization techniques [11], with recent refinements enabling scalable depth reduction through quadratic approximations [5]. Despite these improvements, standard FALQON converges slowly when using conservative fixed hyperparameters, motivating the investigation of adaptive parameter strategies.

Quantum circuits operate under shot-noise limitations, introducing stochastic variation in measurement outcomes. PennyLane [12] and related frameworks enable simulation and optimization of quantum circuits subject to realistic noise models, though real hardware introduces additional error sources including readout errors and crosstalk effects.

B. Quantum Systems and Hamiltonians

A quantum state $|\psi\rangle$ can be understood as a probability distribution over all bitstrings [13]. The Hamiltonian H represents the total energy of a quantum system, and the expected value of the Hamiltonian under state $|\psi\rangle$ is written as $\langle\psi|H|\psi\rangle$ [13]. Time evolution of a state $|\psi_0\rangle$ via Hamiltonian H over time t is governed by the unitary operator [13]:

$$U_H(t) = e^{-iHt} \quad (1)$$

In quantum optimization, two types of Hamiltonians are employed as defined in related literature [3]–[5]: the Problem Hamiltonian (H_p), whose ground states correspond to solutions of the optimization problem and encode the optimization objective, and the Driver Hamiltonian (H_d), chosen to have an easily prepared ground state and to be non-commuting with the Problem Hamiltonian. This non-commutativity relationship ensures a path between ground states exists. Practical implementations of quantum circuits on current hardware exhibit non-negligible gate errors [6], [7], necessitating algorithms that minimize circuit depth.

C. MaxCut Problem and Benchmark

The MaxCut problem is a canonical NP-hard combinatorial optimization problem [14]. Given an undirected simple graph $G = (V, E)$ with $|V| = N$ vertices, the objective is to partition vertices into disjoint sets S and \bar{S} maximizing the number of edges crossing between sets. MaxCut has become the standard benchmark for variational quantum algorithms [3], [14], [15].

For robust statistical evaluation, we employ all non-isomorphic 3-regular graphs with $N = 12$ vertices. A 3-regular graph has degree $d = 3$ for every vertex, containing exactly $|E| = \frac{3N}{2} = 18$ edges. This ensemble comprises precisely 94 distinct graphs under relabeling [16], [17], providing a finite yet diverse benchmark set with well-characterized optimal solutions.

MaxCut is encoded as an Ising Hamiltonian:

$$H_p = \sum_{(i,j) \in E} Z_i Z_j \quad (2)$$

where Z_i is the Pauli-Z operator on qubit i . Minimizing $\langle H_p \rangle$ maximizes the cut value [14].

D. QAOA and Multi-Angle Variants

The Quantum Approximate Optimization Algorithm [3] prescribes parameters $\gamma_k \in \mathbb{R}$ and $\beta_k \in \mathbb{R}$ as unconstrained optimization variables to be optimized via classical methods.

QAOA Multi-Angle (QAOA-MA) [15] extends standard QAOA by replacing scalar parameters with vectors $\vec{\gamma}_k = (\gamma_{k,1}, \dots, \gamma_{k,N_p})$ and $\vec{\beta}_k = (\beta_{k,1}, \dots, \beta_{k,N_d})$, corresponding to individual Hamiltonian components. This expands the parameter space, enabling more expressive ansätze at the cost of increased optimization complexity.

Both gradient-descent and gradient-free optimizers (e.g., Powell) are commonly employed for QAOA parameter tuning. Gradient-free methods show promise in noisy quantum settings where gradient estimates require additional circuit evaluations [18], [19]. Warm-starting QAOA from good initial parameters—such as those derived from other algorithms—has shown empirical benefits [20], [21], motivating investigation of cross-method initialization strategies.

E. Feedback-Based Adaptive Quantum Optimization (FALQON)

FALQON [4], [22] derives a feedback control law requiring only single circuit evaluations per layer, making it exceptionally efficient in terms of evaluation count. This builds on a long tradition of feedback control in quantum systems [23], where control laws adapt parameters based on system measurements. The update rule depends on commutator expectations:

$$A_k = \langle\psi_k|[H_d, H_p]|\psi_k\rangle \quad (3)$$

$$B_k = \langle\psi_k|\frac{1}{2}[[H_d, H_p], H_d]|\psi_k\rangle \quad (4)$$

$$C_k = \langle\psi_k|[[H_d, H_p], H_p]|\psi_k\rangle \quad (5)$$

Standard FALQON applies fixed time step δ and gain $w = 1$ across all layers. Recent extensions introduce per-layer adaptations: time-rescaling modifies the step term and

introduces additional factors which effectively modify the gain term [10], and robust gain regularization scales the gain term using a hyperparameter [11]. These developments suggest that direct layer-wise optimization of both step and scaling parameters could substantially improve practical convergence.

F. Statistical Hypothesis Testing

Comparative algorithm studies require rigorous statistical methodology. The Wilcoxon signed-rank test [24] is a non-parametric test suitable for paired samples lacking normality assumptions [25]. When performing multiple hypothesis tests, family-wise error control via the Holm step-down procedure [26] prevents inflated type-I error rates, ensuring that observed differences are statistically meaningful rather than due to multiple testing.

III. OPTIMAL FALQON METHOD

A. Proposed Formulation

Prior FALQON studies indicate strong convergence sensitivity to step and gain choices, with several extensions prescribing analytical modifications to these terms [4], [5], [10], [11], [22]. We propose treating the per-layer step and scaling terms as decision variables. The symbol M_k is introduced as a unifying scaling term for cross-method comparison. Under this view: standard FALQON corresponds to fixed $\delta_k = \delta$ and $M_k = w$ (typically $w = 1$) [4], [5]; TR-FALQON introduces per-layer rescaling factors that can be interpreted as changes to step and gain terms [10]; robust FALQON uses $w = 1/(2\lambda)$ with $\lambda = 1/2$ recovering the standard $w = 1$ case [11].

The key idea of Optimal FALQON is to optimize these two quantities (step size δ_k and scaling factor M_k) per layer:

$$\delta_k \in \mathbb{R}, \quad k \in [1, L] \quad (6)$$

$$M_k \in \mathbb{R}, \quad k \in [1, L] \quad (7)$$

where L denotes the total number of layers.

For each layer k , we prescribe:

$$\gamma_k = \delta_k \quad (8)$$

$$\beta_k = \begin{cases} -M_k A_{k-1} \delta_k & \text{First Order (FO)} \\ -M_k \left| \frac{A_{k-1} + C_{k-1} \delta_k}{2B_{k-1} \delta_k} \right| \delta_k & \text{Second Order (SO)} \end{cases} \quad (9)$$

where we note that when $|B_{k-1}| < 1 \times 10^{-12}$, the SO method falls back to FO.

The optimization problem is a two-dimensional layer-wise search over $\{\delta_k, M_k\}$ keeping FALQON's structure intact.

B. Classical Optimization and Cost Function

At each layer k , we solve the two-dimensional minimization problem:

$$(\delta_k^*, M_k^*) = \arg \min \text{Cost}_k(\delta_k, M_k) \quad (10)$$

where the cost function is the expected value of the problem Hamiltonian:

$$\text{Cost}_k(\delta_k, M_k) = \langle \psi_k(\delta_k, M_k) | H_p | \psi_k(\delta_k, M_k) \rangle \quad (11)$$

The optimization problem at each layer is:

$$(\delta_k^*, M_k^*) = \arg \min_{\delta_k, M_k} \langle \psi_k(\delta_k, M_k) | H_p | \psi_k(\delta_k, M_k) \rangle \quad (12)$$

We employ the Powell optimizer [18] for its robustness in noisy quantum environments compared to gradient-free alternatives like Nelder-Mead and COBYLA [19]. Existing FALQON variants avoid explicit per-layer optimization loops, but quantum algorithms suffer from multiple noise sources inhibiting optimization [19]. Nelder-Mead [27], Powell, and COBYLA [28] are widely assessed as candidate gradient-free optimizers for noisy optimization landscapes. Powell [18] is recognized as comparatively robust in noisy variational settings with stable and competitive outcomes across noise conditions [19], outperforming Nelder-Mead in our preliminary testing and showing advantages over COBYLA in related quantum benchmarking literature.

C. Benchmarking Framework

We evaluate a systematic suite of algorithms across a comprehensive problem ensemble:

- **FALQON (Standard)**: First-order (FO) with fixed $\delta = 0.03, w = 1$; Second-order (SO) with fixed $\delta = 0.05, w = 1$.
- **Optimal FALQON**: FO and SO variants where δ_k and M_k are optimized per layer using Powell, initialized at $\delta_k = 0.5, M_k = 1$.
- **QAOA Standard**: Initialized with $\gamma = 0.5, \beta = 0.5$; optimized via Gradient Descent or Powell.
- **QAOA Multi-Angle (QAOA-MA)**: Initialized with all $\gamma_{k,j} = 0.5, \beta_{k,j} = 0.5$; optimized via Gradient Descent or Powell.
- **Warm-Started QAOA/QAOA-MA**: Initialized with parameters from standard or Optimal FALQON, then optimized.

Problem instances comprise all 94 non-isomorphic 3-regular graphs with $N = 12$ vertices. Exact optimal solutions were computed via exhaustive search over all $2^{12} = 4096$ bitstrings per instance. Algorithms are evaluated at circuit depths $L \in \{1, 2, 3, \dots, 10\}$ with 8192 shots per evaluation for shot-noise simulation. Hyperparameter settings appear in Table I.

TABLE I: Hyperparameter settings across all method variants and depths.

| Method | Init δ | Init M_k/w | Max Iter | Shots |
|-------------------|---------------|--------------|----------|-------|
| FALQON FO | 0.03 | 1.0 (fixed) | 20 | 8192 |
| FALQON SO | 0.05 | 1.0 (fixed) | 20 | 8192 |
| Optimal FALQON FO | 0.5 | 1.0 | 20 | 8192 |
| Optimal FALQON SO | 0.5 | 1.0 | 20 | 8192 |
| QAOA (GD) | 0.5 | — | 20 | 8192 |
| QAOA-MA (GD) | 0.5 | — | 20 | 8192 |
| QAOA (Powell) | 0.5 | — | 20 | 8192 |
| QAOA-MA (Powell) | 0.5 | — | 20 | 8192 |

D. Performance Metrics

The probability that a single shot samples an optimal Max-Cut solution is:

$$P_{\text{success}} = \sum_{x^{(i)} \in \mathcal{S}^*} P(x^{(i)}) \quad (13)$$

where \mathcal{S}^* denotes the set of all optimal bitstrings for a given graph and $P(x^{(i)})$ is the probability of measuring bitstring $x^{(i)}$ from the quantum state. In practice, we estimate P_{success} by capturing the bitstring probabilities from multi-shot sampling of $|\psi\rangle$ and summing the probabilities of all bitstrings that belong to \mathcal{S}^* .

We define two efficiency metrics to assess cost-performance tradeoffs. Evaluation-normalized efficiency accounts for circuit evaluation count:

$$E_1 = \frac{P_{\text{success}}}{n_{\text{evals}}} \quad (14)$$

Cost-depth efficiency additionally penalizes circuit depth L :

$$E_2 = \frac{P_{\text{success}}}{n_{\text{evals}} \times L} \quad (15)$$

Higher E_1 indicates better use of quantum resources per evaluation. Higher E_2 indicates better joint optimization of both evaluation and depth resources, reflecting realistic NISQ constraints where gate error accumulates with circuit depth.

E. Statistical Methodology

For each metric ($P_{\text{success}}, E_1, E_2$), depth ($L \in \{1, \dots, 10\}$), and method pair, we perform paired Wilcoxon signed-rank tests [24] using all 94 graph instances as matched pairs. The Wilcoxon signed-rank test is a non-parametric test appropriate when normality is not assumed; it tests whether the median paired difference is zero. For background on numerical optimization and statistical testing, see standard computational references [29].

For multiple hypothesis testing, for each metric, the Holm step-down correction [26] was applied across all comparisons in that metric’s test family to control family-wise error at $\alpha = 0.05$. Let N_{tests} denote the number of tests in a comparison family and $p_{(1)} \leq p_{(2)} \leq \dots \leq p_{(N_{\text{tests}})}$ the ordered raw p-values. The Holm-adjusted p-values are:

$$p_{\text{adj},(r)} = \max_{1 \leq u \leq r} [(N_{\text{tests}} - u + 1) p_{(u)}], \quad r = 1, \dots, N_{\text{tests}} \quad (16)$$

with truncation at 1 as needed. A comparison is deemed statistically significant when $p_{\text{adj}} < 0.05$.

IV. SIMULATION RESULTS

A. FALQON Family Results

Figure 1 displays success-probability distributions for FALQON variants across depths $L = 1$ to 10. The dominant pattern is a consistent upward shift for Optimal FALQON variants compared to fixed-parameter FALQON. Standard FALQON achieves median $P_{\text{success}} \sim 0.004$, demonstrating ineffectiveness at utilizing available circuit depth when hyperparameters are conservatively fixed. In contrast, Optimal

FALQON FO and SO achieve median success probabilities approaching 0.22, representing approximately 50-fold improvement.

Figure 2 presents evaluation-normalized efficiency $E_1 = P_{\text{success}}/n_{\text{evals}}$. Optimal FALQON sustains substantially higher E_1 across depths, indicating greater success probability per circuit evaluation. This metric is particularly relevant for NISQ hardware where evaluation cost is a primary economic constraint.

Figure 3 shows depth-normalized efficiency $E_2 = P_{\text{success}}/(n_{\text{evals}} \times L)$. This metric penalizes both evaluation costs and circuit depth, reflecting the dual constraint of gate error accumulation and hardware execution costs. Optimal FALQON maintains substantial efficiency advantage even under this stricter normalization, demonstrating that improvements are not merely artifacts of utilizing more evaluations, but reflect genuine adaptive convergence benefits.

The FALQON family results establish that per-layer optimization of δ_k and M_k yields substantial practical benefits over standard fixed-parameter FALQON.

B. QAOA Family Results: Gradient Descent

Figure 4 shows success probability for QAOA optimized via gradient descent. A clear pattern emerges: warm-starting from Optimal FALQON parameters (whether FO or SO variant) yields substantially higher distributions compared to fixed initialization ($\gamma = 0.5, \beta = 0.5$) or warm-starts from standard FALQON. Median success probability improves from ~ 0.005 (fixed init) and ~ 0.05 (warm start from standard FALQON) to ~ 0.28 (warm start from Optimal FALQON).

Warm-starting QAOA from good initial parameters enables the gradient-based optimizer to explore relevant regions of the parameter space, while fixed initialization often leads to suboptimal local minima. This demonstrates complementarity between feedback-based methods (effective for rapid initial convergence) and classical optimization (effective for fine-tuning in expanded parameter spaces).

C. QAOA Family Results: Powell Optimizer

Figure 5 presents QAOA results using Powell optimization. For this configuration, median P_{success} increased from ~ 0.02 (fixed init) and ~ 0.03 (warm start from standard FALQON) to ~ 0.22 (warm start from Optimal FALQON). Warm-started variants again demonstrate superior performance, though fixed QAOA (Powell) achieves competitive results at specific depths (notably $L = 2$ and $L = 10$), suggesting depth-dependent strengths.

This depth-dependent variation in optimal method suggests that future approaches might employ dynamic algorithm selection, choosing between Optimal FALQON, QAOA, or hybrid methods based on available circuit depth.

D. QAOA-MA Results: Gradient Descent

Figure 6 presents multi-angle QAOA with gradient descent. The expanded parameter space (separate parameters for each Hamiltonian component) provides greater expressiveness, but

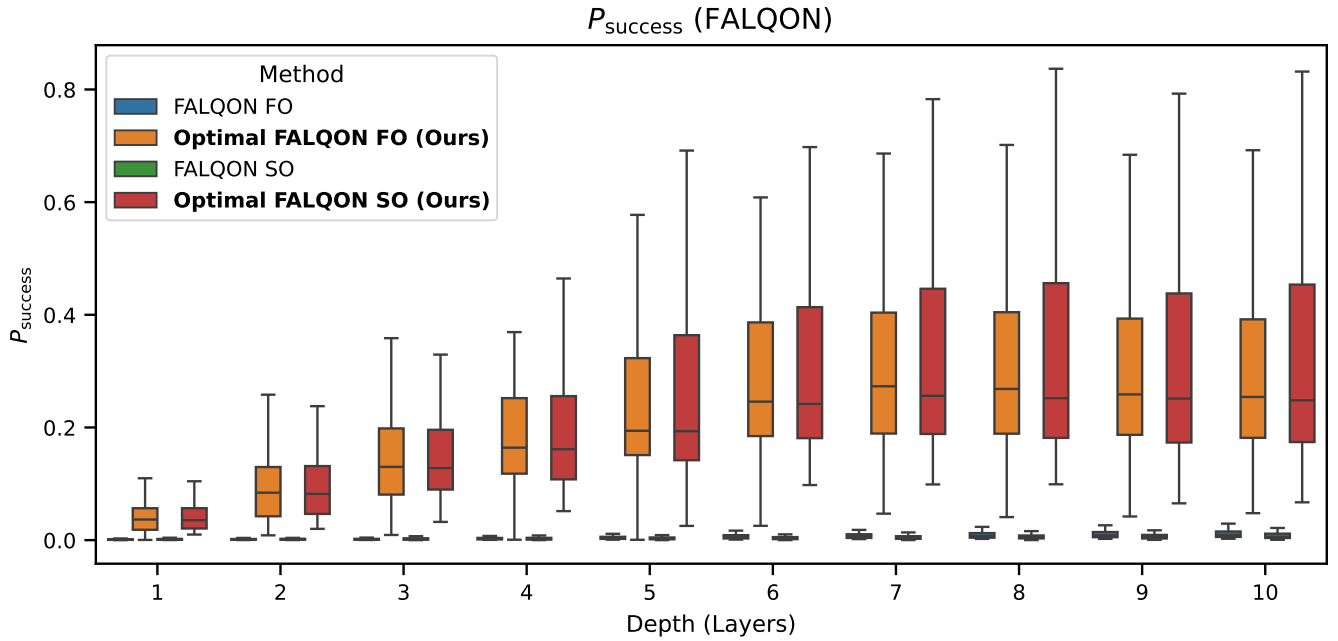


Fig. 1: Depth-wise distributions of P_{success} for FALQON family. Optimal FALQON medians consistently exceed standard FALQON across all depths, with pronounced separation at higher depths.

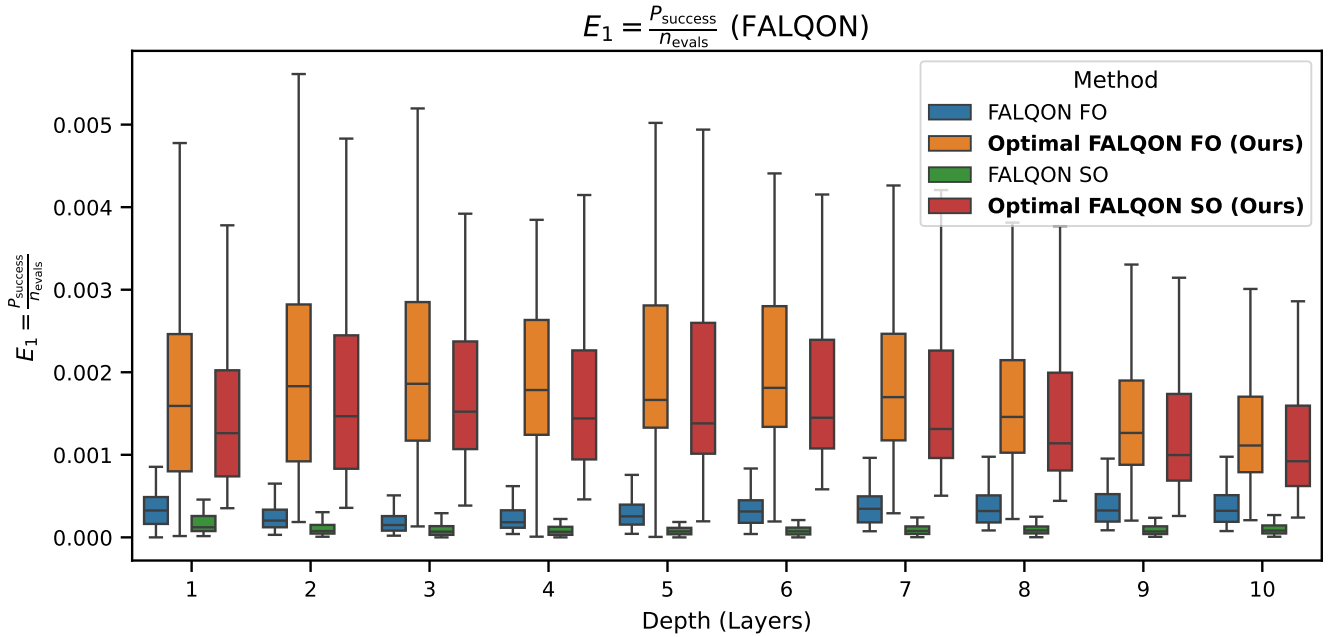


Fig. 2: Depth-wise distributions of E_1 for FALQON variants. Optimal FALQON demonstrates median evaluation-normalized efficiency approximately 5-50 times higher than standard FALQON.

requires stronger initialization guidance to avoid poor local minima. Warm-starting from Optimal FALQON dramatically improves performance: median success probability rises from ~ 0.002 (fixed) and ~ 0.007 (warm-start from standard

FALQON) to ~ 0.22 (warm-start from Optimal FALQON).

E. QAOA-MA Results: Powell Optimizer

Figure 7 shows QAOA-MA with Powell optimization. For this configuration, median P_{success} increases from ~ 0.0001

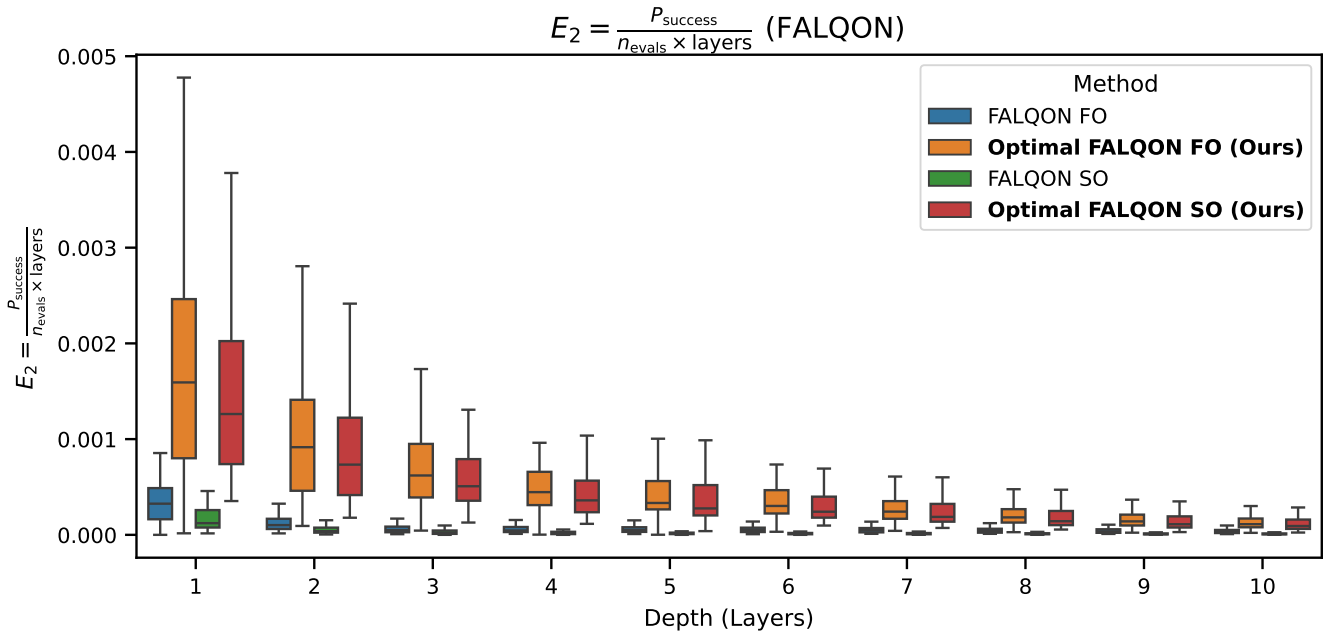


Fig. 3: Depth-wise distributions of E_2 for FALQON variants. Optimal FALQON retains median efficiency advantage after joint evaluation-depth normalization, indicating genuine adaptive benefits.

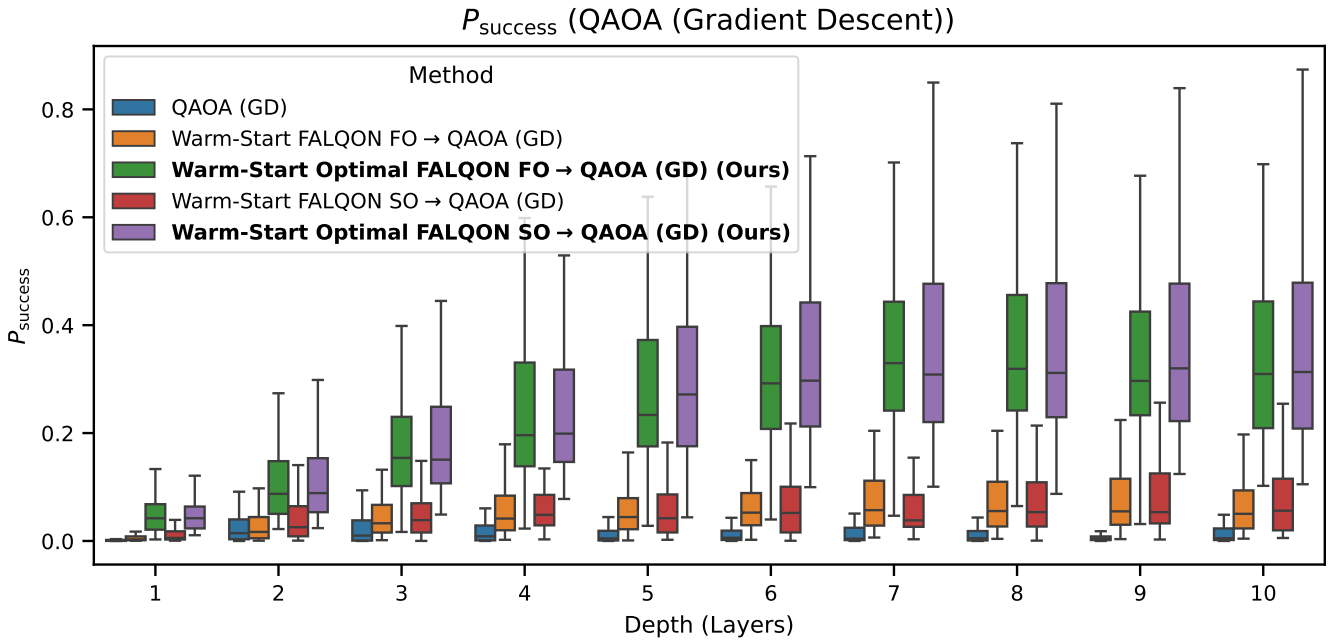


Fig. 4: Depth-wise P_{success} for QAOA with gradient descent. Warm-starting from Optimal FALQON shifts distributions upward relative to fixed initialization and standard FALQON warm-starts.

(fixed init) and ~ 0.003 (warm start from standard FALQON) to ~ 0.27 (warm start from Optimal FALQON).

F. Efficiency Metrics and Cost Analysis

Figure 8 examines evaluation-normalized efficiency E_1 for QAOA (Powell). While warm-started variants dominate at most depths, fixed QAOA (Powell) achieves competitive or

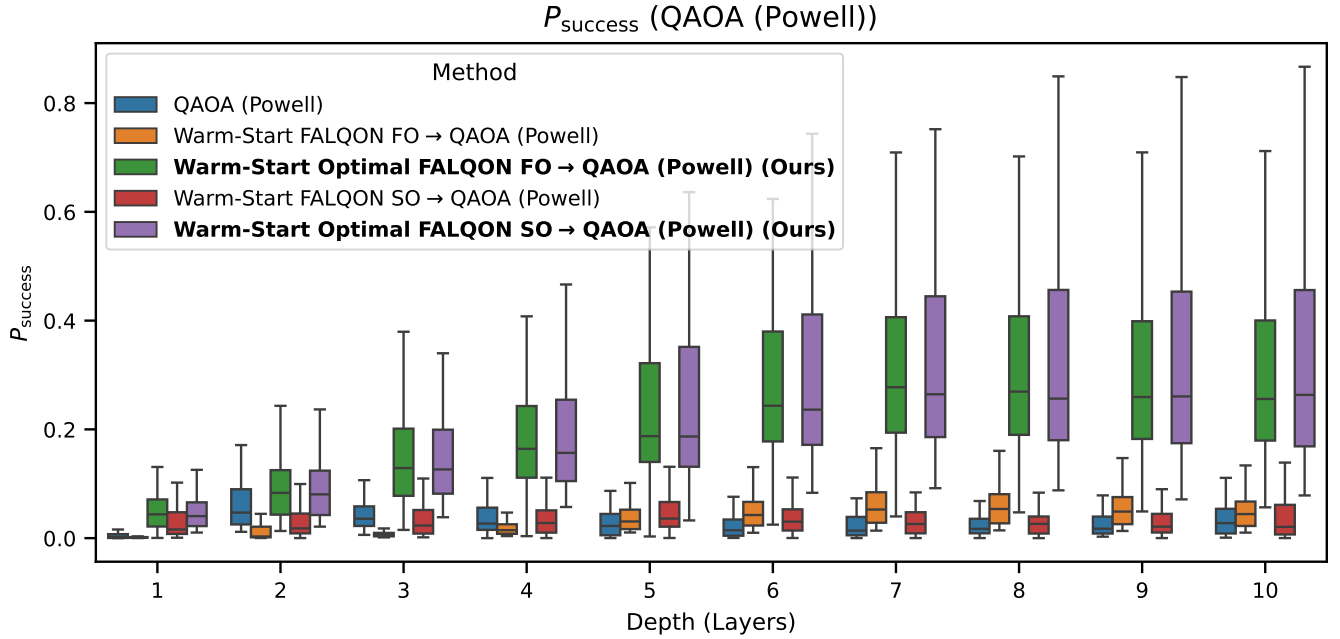


Fig. 5: Depth-wise P_{success} for QAOA with Powell optimizer. Warm-start from Optimal FALQON dominates at most depths; fixed QAOA competitive at isolated depths.

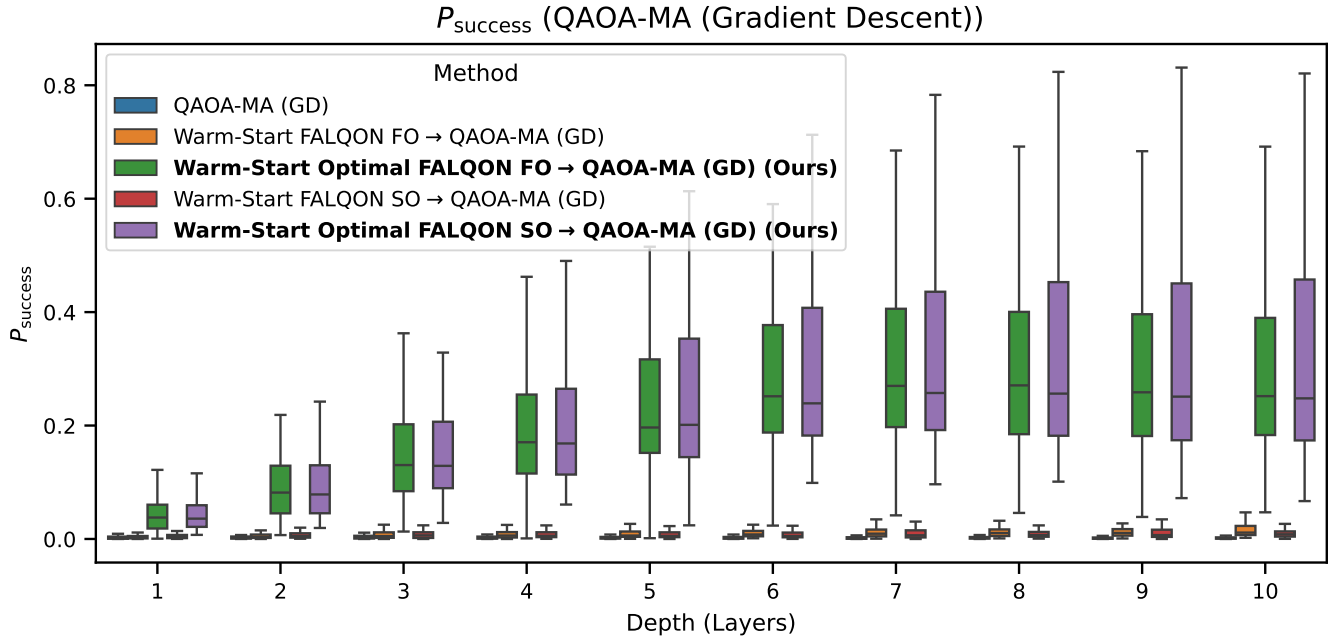


Fig. 6: Depth-wise P_{success} for QAOA-MA with gradient descent. Warm-start from Optimal FALQON shows pronounced advantage over fixed initialization and standard FALQON warm-starts.

superior E_1 at depths $L = 2$ and $L = 10$, revealing depth-dependent efficiency tradeoffs. This suggests that fixed initialization may be sufficient, and further investigations comparing QAOA with and without Optimal FALQON warm start

schedules are warranted.

G. Performance Summary

Table II aggregates median statistics across all depths and 94 graph instances. Optimal FALQON achieves $P_{\text{success}} \approx$

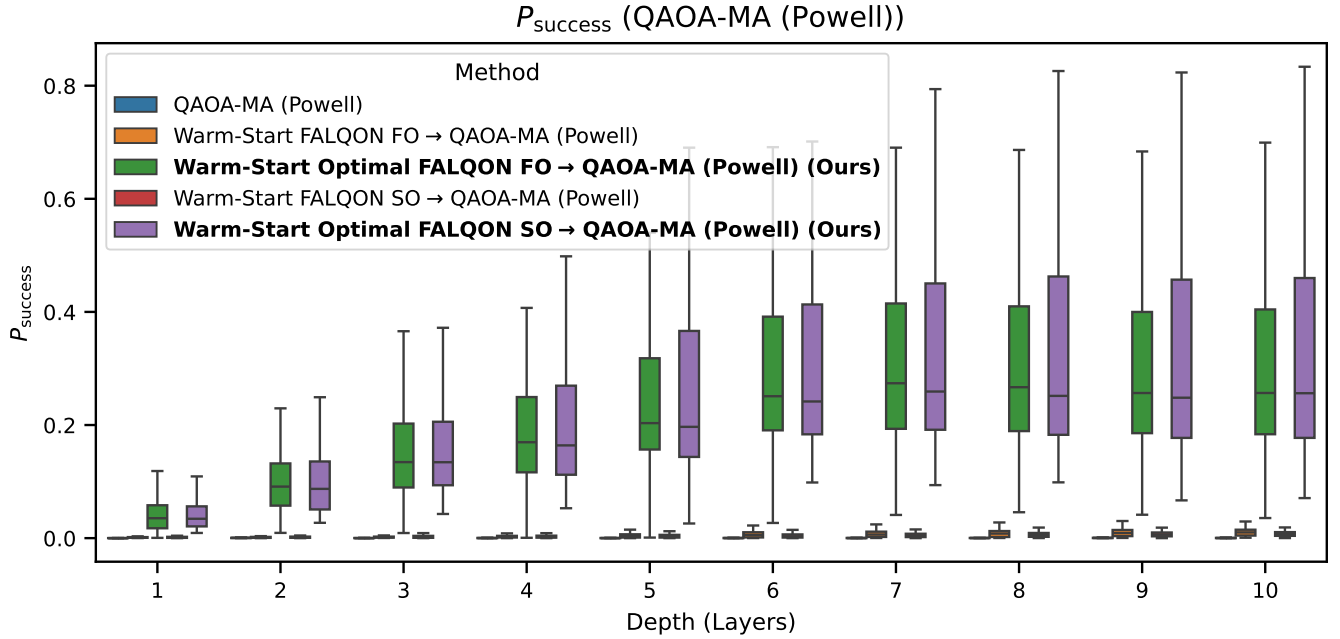


Fig. 7: Depth-wise P_{success} for QAOA-MA with Powell optimizer, demonstrating our method’s effectiveness.

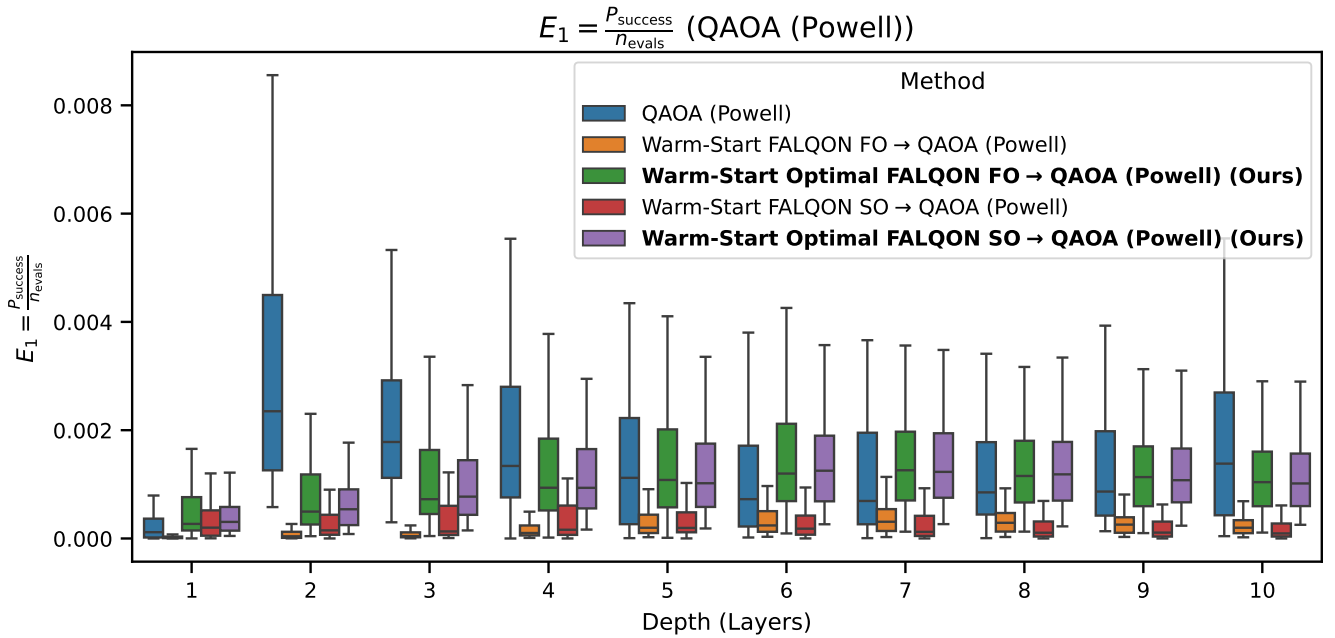


Fig. 8: Depth-wise E_1 efficiency for QAOA (Powell). Optimal FALQON warm-starts maintain high efficiency at most depths; fixed QAOA competitive at $L = 2, 10$.

0.22 compared to standard FALQON’s ~ 0.004 ($50\times$ improvement). In evaluation-normalized efficiency E_1 , Optimal FALQON reaches $1.35\text{--}1.68 \times 10^{-3}$ versus standard FALQON’s $0.07\text{--}0.32 \times 10^{-3}$ ($4\text{--}23\times$ improvement). For depth-aware efficiency E_2 , Optimal FALQON achieves 2.59--

3.17×10^{-4} ($5\text{--}24\times$ improvement over standard FALQON). Warm-starting QAOA (GD) with parameters from the proposed Optimal FALQON yields notably superior success rates (e.g., $0.26\text{--}0.28$), exceeding Optimal FALQON alone, suggesting that gradient descent initialization particularly benefits from feedback-based parameter seeding. Table II reveals that

warm-starting with standard FALQON improves over baseline QAOA (e.g., 0.045–0.047 for QAOA-GD), but warm-starting with the proposed Optimal FALQON provides substantially better results (e.g., 0.263–0.284 for QAOA-GD), demonstrating that layer-wise parameter optimization yields superior initialization values for downstream classical optimization.

H. Statistical Significance Assessment

Comprehensive paired Wilcoxon signed-rank tests with Holm-Bonferroni correction at $\alpha = 0.05$ reveal:

- **Optimal vs. Standard FALQON:** Optimal FALQON exhibits statistically significant superiority ($p_{\text{adj}} < 0.05$) in P_{success} , E_1 , and E_2 across nearly all depths. This dominant pattern confirms that layer-wise parameter optimization provides substantial benefits.
- **FO vs. SO within Optimal FALQON:** The two variants are frequently statistically indistinguishable in terms of P_{success} ($p_{\text{adj}} > 0.05$), indicating that first-order optimization captures most benefits without the additional measurement overhead of second-order methods. For practitioners, FO is recommended.
- **Warm-Start Benefits:** Initialization with Optimal FALQON parameters yields statistically significant improvements across QAOA and QAOA-MA variants compared to fixed initialization and warm-starts from standard FALQON.
- **Depth-Dependent Effects:** Fixed QAOA (Powell) achieves statistical equivalence to warm-started variants at specific depths, indicating depth-dependent algorithm selection opportunities. This suggests future work should explore adaptive method selection.

V. DISCUSSION

The empirical study validates several key insights about adaptive quantum optimization:

a) Dynamic Per-Layer Tuning Effects: Optimizing δ_k and M_k yields clear performance benefits over static standard FALQON. The 50-fold improvement in success probability (0.22 vs. 0.004) indicates that adaptive step sizes enable layers to move closer to optimal gradient directions, mitigating overshoot and undershoot effects that plague fixed-step schemes. This aligns with the observation in prior FALQON literature that convergence sensitivity to parameter choices is a critical limitation.

b) First-Order vs. Second-Order Trade-Off: While the SO variant uses more accurate gradient estimates from commutator expectations B_k and C_k , its practical advantage over FO is marginal ($p_{\text{adj}} > 0.05$ in most comparisons). The additional measurement overhead required to estimate B_k and C_k does not translate to statistically significant performance gains. For practitioners, FO Optimal FALQON is recommended, achieving most adaptive benefits with reduced measurement burden.

c) Warm-Start Synergies: Initializing QAOA/QAOA-MA with Optimal FALQON parameters produces substantial improvements over fixed initialization and standard FALQON warm-starts. The highest overall success rate ($P_{\text{success}} \approx 0.28$) occurs with warm-started QAOA-MA (GD). This suggests that combining structured parameter guidance from feedback-based methods with classical optimization creates complementary benefits: FALQON provides rapid convergence in early layers, while QAOA refines parameters in expanded spaces.

d) Depth-Dependent Method Selection: Fixed QAOA (Powell) achieves competitive or superior performance at specific depths (particularly $L = 2, 10$), while warm-started variants dominate at other depths. This depth-dependence suggests future work should explore adaptive method selection strategies that choose algorithms and warm-start sources based on available circuit depth.

e) Practical Implications: On current NISQ hardware with execution costs of \$10 per evaluation, the evaluation efficiency gains translate directly to cost reductions. Optimal FALQON enables cost-per-solution reductions of nearly 1 order of magnitude, making quantum optimization more economically viable for practical applications.

VI. CONCLUSION

This paper introduces Optimal FALQON, an optimization-based extension of FALQON that treats per-layer time step (δ_k) and scaling parameters (M_k) as decision variables solved via Powell optimization. Comprehensive evaluation on all 94 non-isomorphic 3-regular graphs with 12 vertices—across multiple QAOA variants, depths 1–10, and both first-order and second-order formulations—demonstrates:

- **Significant Improvements:** Optimal FALQON achieves 50-fold improvement in success probability over standard FALQON, with statistically significant gains across multiple efficiency metrics.
- **Reduced Computational Cost:** Optimal FALQON median $E_1 \approx 1.4\text{--}1.7\times$ higher than baseline QAOA (Powell) and $\approx 5\text{--}50\times$ higher than baseline QAOA (GD) translate to substantial cost savings on current NISQ hardware.
- **Warm-Start Synergies:** Hybrid approaches warm-starting QAOA with Optimal FALQON parameters achieve the highest overall success rates, demonstrating complementary benefits of feedback-based and classical optimization.
- **Statistical Rigor:** Paired Wilcoxon tests with Holm correction provide robust evidence of method superiority, while revealing that FO and SO variants are frequently equivalent in terms of P_{success} , simplifying practical deployment.

The practical applicability is strong: per-layer optimization imposes minimal overhead (20 evaluations per layer in our implementation) while yielding substantial performance gains. The method is readily implementable in modern quantum computing frameworks (PennyLane, Qiskit) and scales naturally to larger problems.

TABLE II: Overall median performance aggregating all depths and 94 instances. Metrics: success probability P_{success} , evaluation efficiency E_1 , depth-normalized efficiency E_2 . Optimal FALQON methods shown in bold.

| Method | Med P_{succ} | Med $E_1 \times 10^{-3}$ | Med $E_2 \times 10^{-4}$ |
|---|-----------------------|--------------------------|--------------------------|
| FALQON FO | 4.39×10^{-3} | 0.32 | 0.50 |
| Optimal FALQON FO | 2.20×10^{-1} | 1.68 | 3.17 |
| FALQON SO | 3.11×10^{-3} | 0.07 | 0.13 |
| Optimal FALQON SO | 2.18×10^{-1} | 1.35 | 2.59 |
| QAOA (GD) | 5.04×10^{-3} | 0.04 | 0.058 |
| QAOA (Powell) | 1.99×10^{-2} | 0.99 | 1.30 |
| Warm-Start FALQON FO \rightarrow QAOA (GD) | 4.73×10^{-2} | 0.22 | 0.42 |
| Warm-Start Optimal FALQON FO \rightarrow QAOA (GD) | 2.63×10^{-1} | 0.93 | 1.87 |
| Warm-Start FALQON SO \rightarrow QAOA (GD) | 4.52×10^{-2} | 0.24 | 0.45 |
| Warm-Start Optimal FALQON SO \rightarrow QAOA (GD) | 2.84×10^{-1} | 1.02 | 2.05 |
| Warm-Start FALQON FO \rightarrow QAOA (Powell) | 3.66×10^{-2} | 0.18 | 0.23 |
| Warm-Start Optimal FALQON FO \rightarrow QAOA (Powell) | 2.16×10^{-1} | 0.97 | 1.86 |
| Warm-Start FALQON SO \rightarrow QAOA (Powell) | 2.47×10^{-2} | 0.16 | 0.34 |
| Warm-Start Optimal FALQON SO \rightarrow QAOA (Powell) | 2.12×10^{-1} | 1.01 | 1.99 |
| QAOA-MA (GD) | 1.65×10^{-3} | 0.004 | 0.007 |
| QAOA-MA (Powell) | 1.22×10^{-4} | 0.002 | 0.002 |
| Warm-Start FALQON FO \rightarrow QAOA-MA (GD) | 7.00×10^{-3} | 0.04 | 0.08 |
| Warm-Start Optimal FALQON FO \rightarrow QAOA-MA (GD) | 2.24×10^{-1} | 0.81 | 1.63 |
| Warm-Start FALQON SO \rightarrow QAOA-MA (GD) | 5.92×10^{-3} | 0.03 | 0.05 |
| Warm-Start Optimal FALQON SO \rightarrow QAOA-MA (GD) | 2.20×10^{-1} | 0.89 | 1.82 |
| Warm-Start FALQON FO \rightarrow QAOA-MA (Powell) | 4.88×10^{-3} | 0.02 | 0.04 |
| Warm-Start Optimal FALQON FO \rightarrow QAOA-MA (Powell) | 2.27×10^{-1} | 0.94 | 1.93 |
| Warm-Start FALQON SO \rightarrow QAOA-MA (Powell) | 2.93×10^{-3} | 0.02 | 0.03 |
| Warm-Start Optimal FALQON SO \rightarrow QAOA-MA (Powell) | 2.19×10^{-1} | 1.02 | 2.01 |

We anticipate Optimal FALQON will be valuable for near-term quantum optimization on NISQ devices, where circuit depth and evaluation budgets are severely constrained and computational cost is a primary concern.

REFERENCES

- [1] A. Peruzzo, J. McClean, P. Shadbolt, M.-H. Yung, X.-Q. Zhou, P. J. Love, A. Aspuru-Guzik, and J. L. O’Brien, “A variational eigenvalue solver on a photonic quantum processor,” *Nature Communications*, vol. 5, p. 4213, 2014. [Online]. Available: <https://doi.org/10.1038/ncomms5213>
- [2] J. R. McClean, J. Romero, R. Babbush, and A. Aspuru-Guzik, “The theory of variational hybrid quantum-classical algorithms,” *New Journal of Physics*, vol. 18, p. 023023, 2016. [Online]. Available: <https://doi.org/10.1088/1367-2630/18/2/023023>
- [3] E. Farhi, J. Goldstone, and S. Gutmann, “A quantum approximate optimization algorithm,” *arXiv preprint arXiv:1411.4028*, 2014. [Online]. Available: <https://arxiv.org/abs/1411.4028>
- [4] A. B. Magann, K. M. Rudinger, M. D. Grace, and M. Sarovar, “Feedback-based quantum optimization,” *Physical Review Letters*, vol. 129, p. 250502, 2022. [Online]. Available: <https://doi.org/10.1103/PhysRevLett.129.250502>
- [5] D. Arai, K. N. Okada, Y. Nakano, K. Mitarai, and K. Fujii, “Scalable circuit depth reduction in feedback-based quantum optimization with a quadratic approximation,” *Physical Review Research*, vol. 7, p. 013035, Jan 2025. [Online]. Available: <https://doi.org/10.1103/PhysRevResearch.7.013035>
- [6] F. Arute, K. Arya, R. Babbush *et al.*, “Quantum supremacy using a programmable superconducting processor,” *Nature*, vol. 574, no. 7779, pp. 505–510, 2019. [Online]. Available: <https://doi.org/10.1038/s41586-019-1666-5>
- [7] M. Kjaergaard, M. E. Schwartz, J. Braumüller, P. Krantz, J. I.-J. Wang, S. Gustavsson, and W. D. Oliver, “Superconducting qubits: Current state of play,” *Annual Review of Condensed Matter Physics*, vol. 11, no. 1, pp. 369–395, 2020. [Online]. Available: <https://doi.org/10.1146/annurev-conmatphys-031119-050605>
- [8] IBM Research, “Ibm quantum services,” <https://www.ibm.com/quantum>, 2025, accessed: January 24, 2026.
- [9] Amazon Web Services, “Amazon braket pricing,” <https://aws.amazon.com/braket/pricing/>, 2026, accessed: January 24, 2026.
- [10] L. A. M. Rattighieri, G. E. L. Peixe, B. L. Bernardo, and F. F. Fanchini, “Accelerating feedback-based quantum algorithms through time rescaling,” *Physical Review A*, vol. 112, p. 042607, 2025. [Online]. Available: <https://doi.org/10.1103/PhysRevA.112.042607>
- [11] M. Legnini and J. Berberich, “Robust feedback-based quantum optimization: analysis of coherent control errors,” in *2025 IEEE International Conference on Quantum Control, Computing and Learning (qCCL)*, 2025, pp. 17–22. [Online]. Available: <https://doi.org/10.1109/qCCL65142.2025.11158422>
- [12] V. Bergholm, J. Izaac, M. Schuld, C. Gogolin, C. Blank, K. McKiernan, and N. Killoran, “Pennylane: Automatic differentiation of hybrid quantum-classical computations,” *arXiv preprint arXiv:1811.04968*, 2018.
- [13] D. J. Griffiths and D. F. Schroeter, *Introduction to Quantum Mechanics*, 3rd ed. Cambridge University Press, 2018.
- [14] M. H. M. noz Arias, S. Kourtis, and A. Blais, “Low-depth clifford circuits approximately solve maxcut,” *Physical Review Research*, vol. 6, p. 023294, 2024. [Online]. Available: <https://doi.org/10.1103/PhysRevResearch.6.023294>
- [15] R. Herrman, P. C. Lotshaw, J. Ostrowski, T. S. Humble, and G. Siopsis, “Multi-angle quantum approximate optimization algorithm,” *Scientific Reports*, vol. 12, p. 6781, 2022. [Online]. Available: <https://doi.org/10.1038/s41598-022-10555-8>
- [16] The Sage Developers, *SageMath, the Sage Mathematics Software System (Version 9.5)*, 2022, <https://www.sagemath.org>.
- [17] B. D. McKay, “Practical graph isomorphism,” *Congressus Numerantium*, vol. 30, pp. 45–87, 1981, version 2.7: <https://pallini.di.uniroma1.it/>.
- [18] M. J. D. Powell, “An efficient method for finding the minimum of a function of several variables without calculating derivatives,” *The Computer Journal*, vol. 7, no. 2, pp. 155–162, 1964.
- [19] M. A. Alam, S. Ghosh, T. S. Humble, and N. Imam, “A comparison of various classical optimizers for a variational quantum linear solver,” *arXiv preprint arXiv:2106.08682*, 2021.
- [20] D. J. Egger, J. Mareček, and S. Woerner, “Warm-starting quantum optimization,” *Quantum*, vol. 5, p. 479, jun 2021. [Online]. Available: <https://doi.org/10.22331/q-2021-06-17-479>
- [21] S. H. Sack and M. Serbyn, “Quantum annealing initialization of the quantum approximate optimization algorithm,” *Quantum*, vol. 5, p. 491, jul 2021. [Online]. Available: <https://doi.org/10.22331/q-2021-07-01-491>

- [22] A. B. Magann, K. M. Rudinger, M. D. Grace, and M. Sarovar, "Lyapunov control-inspired strategies for quantum combinatorial optimization," *Physical Review A*, vol. 106, p. 062414, 2022. [Online]. Available: <https://doi.org/10.1103/PhysRevA.106.062414>
- [23] S. Grivopoulos and B. Bamieh, "Lyapunov-based control of quantum systems," in *Proceedings of the 42nd IEEE Conference on Decision and Control*, vol. 1. Maui, HI, USA: IEEE, dec 2003, pp. 434–438.
- [24] F. Wilcoxon, "Individual comparisons by ranking methods," *Biometrics Bulletin*, vol. 1, no. 6, pp. 80–83, 1945.
- [25] M. Hollander, D. A. Wolfe, and E. Chicken, *Nonparametric Statistical Methods*, 3rd ed. Wiley, 2013.
- [26] S. Holm, "A simple sequentially rejective multiple test procedure," *Scandinavian Journal of Statistics*, vol. 6, pp. 65–70, 1979.
- [27] J. A. Nelder and R. Mead, "A simplex method for function minimization," *The Computer Journal*, vol. 7, no. 4, pp. 308–313, 1965.
- [28] M. J. D. Powell, "A direct search optimization method that models the objective and constraint functions by linear interpolation," in *Advances in Optimization and Numerical Analysis*. Springer, 1994, pp. 51–67.
- [29] The Scipy community, *Scipy Lecture Notes*, https://scipy-lectures.org/advanced/mathematical_optimization/, 2023, <https://scipy-lectures.org/>.